Technical report 16-008

Fuel cell cars in a microgrid for synergies between hydrogen and electricity networks*

F. Alavi, E. Park Lee, N. van de Wouw, B. De Schutter, and Z. Lukszo

Fuel cell cars in a microgrid for synergies between hydrogen and electricity networks

Farid Alavi[a,*], Esther Park Lee[b], Nathan van de Wouw[a,**], Bart De Schutter[a], Zofia Lukszo[b]

[a]*Delft Center for Systems and Control, Delft University of Technology*
[b]*Faculty of Technology, Policy and Management, Delft University of Technology*

Abstract

Fuel cell electric vehicles convert chemical energy of hydrogen into electricity to power their motor. Since cars are used for transport only during a small part of the time, energy stored in the on-board hydrogen tanks of fuel cell vehicles can be used to provide power when cars are parked. In this paper, we present a community microgrid with photovoltaic systems, wind turbines, and fuel cell electric vehicles that are used to provide vehicle-to-grid power when renewable power generation is scarce. Excess renewable power generation is used to produce hydrogen, which is stored in a refilling station. A central control system is designed to operate the system in such a way that the operational costs are minimized. To this end, a hybrid model for the system is derived, in which both the characteristics of the fuel cell vehicles and their traveling schedules are considered. The operational costs of the system are formulated considering the presence of uncertainty in the prediction of the load and renewable energy generation. A robust min-max model predictive control scheme is developed and finally, a case study illustrates the performance of the designed system.

Keywords: Energy management systems, vehicle-to-grid, hybrid systems

1. Introduction

Power systems are accommodating an increasing amount of renewable generation. However, Renewable Energy Sources (RES) such as the sun or the wind are variable, uncertain and not dispatchable, and therefore electricity is not always produced when it is needed by the users. Flexibility sources like dispatchable generation, storage, demand side response, and increased interconnection are needed to integrate more renewable power generation to power systems [1, 2].

Electric Vehicles (EVs) can provide the flexibility needed in future electric power systems. Although plug-in EVs represent a new source of variability due to their charging needs, this variability can be managed via smart charging

---
[*]Corresponding author
[**]Nathan van de Wouw is also with the Department of Mechanical Engineering, Eindhoven University of Technology, The Netherlands, and the Department of Civil, Environmental & Geo-Engineering, University of Minnesota, Minneapolis, U.S.A.

strategies [3], and the vehicles' batteries can also be used to store surplus renewable generation. Moreover, plug-in EVs can become dispatchable power plants by providing power or balancing services via vehicle-to-grid (V2G) technology [4]. Fuel Cell Electric Vehicles (FCEVs), with hydrogen as fuel, can be used to support the operation of power systems with a large participation of RES. They are particularly suited to provide peak power or spinning reserves to the grid [5, 6]. Because they use hydrogen as a fuel, they do not draw power from the grid, and if aggregated, they can provide large amounts of power. In contrast to plug-in EVs, if FCEVs have a connection to a hydrogen source, they can be operated continuously regardless of the level of fuel stored in their tank [5]. Through the use of FCEVs for both transportation and power generation, we can explore the synergies that can be created between hydrogen and electricity networks.

In this paper, we present the Car as Power Plant (CaPP). This concept, originating from van Wijk, is extensively described in [7]. CaPP introduces a flexible multi-modal energy system that uses FCEVs as dispatchable power plants [8]. It is based on the fact that FCEVs, when parked, can produce electricity from hydrogen in a cleaner and more efficient way than the current power system, thereby producing waste products (water and heat) that can be re-used [7, 9]. Since cars are used for driving only around 5% of the time, there is a big potential to replace peak power plants with a large fleet of FCEVs or to reduce the need to build new plants in the future. Additionally, heat generated in the fuel cells can be used locally if the FCEVs are connected directly to a building's heat network [6].

The CaPP concept can be implemented in different settings and for different types of applications. When applied in a parking lot, a large fleet of parked cars can be used to provide power to the grid through an aggregator that sells power on behalf of the drivers. In residential microgrid settings, residents of the neighborhood can use their FCEVs to provide power to the local grid at times of low renewable power generation. In buildings with high electricity and heat demand, such as hospitals, the CaPP system can be implemented not only to use the electricity and heat from vehicles, but also to provide a large back-up capacity to the building.

In the current paper, we explore the possible synergies between hydrogen and electricity networks using the residential microgrid CaPP case. We consider a residential microgrid with distributed generators that are used to serve local loads and to produce hydrogen, which acts as energy storage medium. This gaseous fuel is used by cars to drive, and additionally, it can be used to generate power when renewable power sources are scarce. This system is studied from the operational control perspective, as operational control is one of the main challenges in the implementation of microgrids [10].

The operational control aspects to take into account in the CaPP microgrid are the scheduling of the FCEVs and the electrolyzer in the power-to-gas (P2G) system. In the literature, the scheduling problem of grid-integrated vehicles in microgrids is usually addressed with centralized optimization approaches, where the resources from plug-in EVs are managed by minimizing power losses in the system [11] or by minimizing the operating costs [12]. In a microgrid with renewable resources, a power-to-gas (P2G) system and vehicle-to-grid (V2G) power from FCEVs, the V2G scheduling problem is addressed by minimizing the power imported from the grid [13]. The operation of electrolyzers in P2G

systems is also addressed with optimization approaches in the literature [14, 15, 16]. Similar control objectives are used, for example, maximizing the profits from wind power export to the grid while taking into account the hydrogen demand [14]. In [17] the sizing and techno-economic aspects of a PV-to-hydrogen system with fuel cell buses are studied using a simple control algorithm.

Model predictive control is used in the operation of microgrids in [18]. The optimization problem in [18] is formulated as a mixed integer linear programming problem. Herein, it is assumed that the prediction of the electrical load of the microgrid is accurate and there is no uncertainty in the system. To deal with the uncertainty in the prediction of the load and generation of renewable energy sources, robust control techniques are developed in [19] and [20]. A stochastic optimization approach is used in [19] where a set of scenarios are selected for the uncertainty in the system. However, the selection of a reliable set is not always possible. In [20], the authors develop a min-max optimization method to operate a microgrid. However, the use of the fuel cells and electrolyzer, in addition to the connection of the microgrid to the power grid and exchange of electricity is not considered in [20].

In this paper, a model is developed that describes the power generation of the fuel cell cars while the transportation aspect of the cars is taken into account. Further, a unified model is derived that describes the economic dispatch problem of a microgrid including a fleet of fuel cell cars, a water electrolysis system, and RES in the form of wind turbines and PV systems. A model predictive control scheme is developed to govern the system operation while the uncertainty in the prediction of the electrical load and power generation of RES is taken into account. The min-max optimization problem that arises in model predictive control is converted into a mixed integer linear programming problem. Realistic data for the behavior of drivers based on the survey of the Dutch Ministry of Infrastructure and renewable energy generation based on the Dutch weather data are used to illustrate the behavior of the system.

The rest of the paper is organized as follows: In Section 2 we describe the CaPP microgrid system. In Section 3 the system model is developed. Section 4 develops an optimization problem to be used in the control system. In Section 5, a case study is simulated and, finally, Section 6 concludes the paper.

2. The CaPP microgrid system

2.1. Description of the system

The CaPP microgrid consists of a group of residential loads, a PV system, a wind turbine, an electrolyzer, and a hydrogen storage system, as depicted in Figure 1. A centralized PV system and also a wind turbine are used to provide electricity to the households. When there is a surplus of renewable power generation, it is used to produce hydrogen via electrolysis of water. The hydrogen produced is compressed and stored in a central storage tank, which is used as a refilling station for FCEVs. The FCEVs are used both for the transportation of residents of the neighborhood and also the generation of electricity inside the neighborhood. The energy management system controls the flows of electricity and the scheduling of FCEVs as power plants.

A side product of generating electricity in each fuel cell stack is heat. In order to keep the temperature of the fuel cell stack inside the desired range,

FCEVs are equipped with a relatively big radiator and cooling fans. We assume that in the stationary mode, when the FCEVs are used to generate electricity for the microgrid, the fuel cells are only operated at partial load. In other words, the maximum power generation of a fuel cell in the stationary mode would be a small fraction of its nominal power. As a result, the on-board utilities of an FCEV would be still able to regulate the fuel cell's temperature, even at standstill. It is worth mentioning that the use of waste heat from the vehicles can be accommodated by heat exchange equipment suggested by [6]. Others like [5] reject the idea given the additional equipment needed and complexity involved, but this could be solved by centralizing the heat exchange system. However, in this paper, we focus on the electrical power generated by the fuel cells. The use of the fuel cell's heat and their corresponding models is considered as a topic for future research.
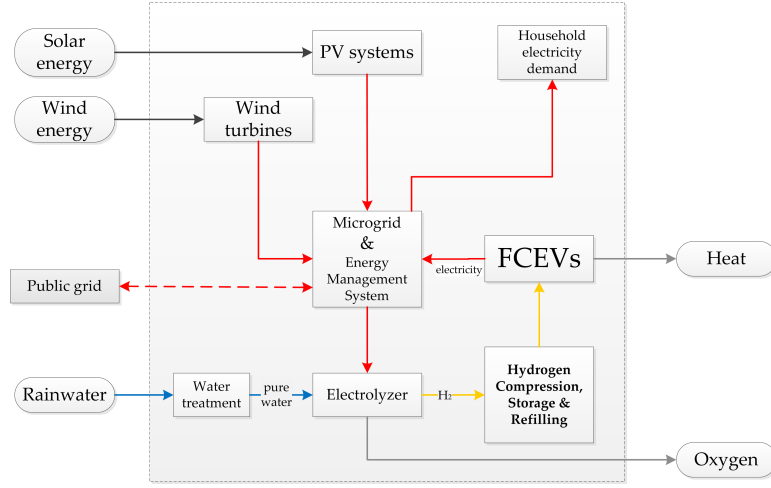

Figure 1: Schematic presentation of the CaPP microgrid system.

A common feature in most of the RES, such as wind and solar energy, is the variation in power generation due to fluctuations in the weather conditions. The CaPP concept brings the opportunity to create a microgrid system with RES and without wind and solar energy curtailment. We assume that the microgrid is connected to the power grid and that exchange of electrical power may happen in both directions. It is assumed that the cost of power exchange between the microgrid and the power grid is determined by the power grid operator. Based on the load and the generation profile of the other generation units in the power network, the power grid operator may determine a reward for the microgrid to export power to the grid. However, in some other situations, the power grid operator may discourage the microgrid for exporting the power by determining a cost for the exported power. The existence of the fuel cell cars and water electrolysis system create the flexibility for the microgrid to set the power exchange with the power grid in such a way that the maximum benefit is gained for the microgrid.

4

The implementation of the CaPP microgrid system will be beneficial for the transportation system. The CaPP microgrid would provide FCEVs with renewable hydrogen, reducing not only the tailpipe emissions of the transportation system, but also the well-to-wheel emissions. In addition, such a microgrid will benefit from storage of excess renewable generation in the form of hydrogen, increasing the system's flexibility and capturing better the renewable generation potential. Finally, using FCEVs to provide power in the microgrid will increase the system's flexibility in power generation. When FCEVs are operated as power plants using hydrogen that was produced from renewable electricity, the overall carbon emissions linked to the electricity consumption in the microgrid will also be low. Without the vehicles in the microgrid, other dispatchable power plants, demand response, and storage should be used. Alternatively, electricity has to be imported from the public grid at times of low or no renewable generation.

3. Modeling the CaPP microgrid

In this section, the CaPP microgrid system is modeled. To this end, first we develop a hybrid model that describes the behavior of the fuel cell cars and, next, with a similar approach, the hybrid model of the electrolysis system and the hydrogen storage tank is developed.

3.1. Fuel cell cars model

The fuel cell cars are considered as controllable power generation units. We assume that the total number of cars in the microgrid is equal to N_{veh}. Let $x_{\text{f},i}(k)$ represent the amount of fuel level in the car number i at time step k. The inputs of the model consist of a continuous variable, $u_{\text{f},i}(k)$, and two binary variables, $s_{\text{f},i}(k)$ and $s_{\text{r},i}(k)$ for each fuel cell car i. The value of $u_{\text{f},i}(k)$ determines the net power generation of fuel cell car i at time step k. It is assumed that a lower-level control system exists in each fuel cell car that can operate the fuel cell stack of the car in such a way that the net power generation of the car is equal to a given set-point, $u_{\text{f},i}(k)$. The value of the binary variable $s_{\text{f},i}(k)$ determines the operation mode of the fuel cell of car i at time step k. If $s_{\text{f},i}(k) = 1$, the fuel cell is turned on; if $s_{\text{f},i}(k) = 0$, the fuel cell is turned off. In addition, the refilling process of the cars is determined based on the value of $s_{\text{r},i}(k)$, where $s_{\text{r},i}(k) = 1$ indicates that the car i is refilled at time step k.

The fuel level of the car i, when its fuel cell is turned on, can be described by [21, 22]

$$x_{\text{f},i}(k+1) = x_{\text{f},i}(k) - (\alpha_{\text{f},i}u_{\text{f},i}(k) + \beta_{\text{f},i})T_{\text{s}}, \tag{1}$$

where $\alpha_{\text{f},i}$ and $\beta_{\text{f},i}$ are two parameters related to the specifications of each fuel cell stack i. The sampling time interval of the system is presented by T_{s}.

The model presented in this paper includes both the trip characteristics and the power generation of the cars. Trip characteristics of the cars are the information about the estimated departure and arrival time of each car, in addition to the distance that each car has traveled. The availability of each car in the task of power generation is determined by the trip characteristics. If a car leaves the neighborhood at a specific time, it will not be available in the

process of electricity generation until it comes back. In addition, an amount of fuel will be used during the travel of the car. In this paper, we assume that the trip characteristics of the cars are not controllable, but predictable. Even though the predictions of the departure and arrival time of the cars are not completely accurate, it is possible to determine tight but guaranteed lower bounds for the departure times of each car. Similarly, we can determine tight but guaranteed upper bounds for the arrival times of each car. As a result, there is no uncertainty in the trip characteristics of the cars.

A binary number, $\lambda_{\mathrm{f},i}(k)$, indicates whether fuel cell car i is available in the neighborhood at time step k. In addition, the amount of fuel that is used during the travel of car i is denoted by $h_i(k)$. It is assumed that if fuel cell car i leaves the neighborhood and comes back again at time step k, the value of $h_i(k)$ represents the amount of fuel that is used for this transportation. For all other values of k, we set $h_i(k) = 0$.

The model of fuel cell car i including the refilling process and the trip characteristics of the car is as follows:

$$x_{\mathrm{f},i}(k+1) = \begin{cases} x_{\mathrm{f},i}(k) + R_{\mathrm{f},i} & \text{refilling} \\ x_{\mathrm{f},i}(k) & \text{no generation} \\ x_{\mathrm{f},i}(k) - (\alpha_{\mathrm{f},i} u_{\mathrm{f},i}(k) + \beta_{\mathrm{f},i}) T_{\mathrm{s}} & \text{generation} \\ x_{\mathrm{f},i}(k) & \text{transportation} \\ x_{\mathrm{f},i}(k) - h_i(k) & \text{arrival,} \end{cases} \qquad (2)$$

where $R_{\mathrm{f},i}$ represents the rate of fuel that can be injected to fuel cell car i during the process of refilling. The model in (2) is a hybrid piecewise affine (PWA) model with five modes. The refilling mode represents a case that the car is being refilled. The no generation mode is related to the case that the car is available for the task of power generation, but it is switched off. Similarly, the generation mode indicates that the car is available and it is switched on. The transportation mode relates to the case that the car is not in the neighborhood. Finally, the arrival mode is related to the arrival time of the car. A full description of each mode and the operational constraints are given in Appendix A.

3.2. Electrolysis system model

A water electrolysis system is responsible for providing the hydrogen needed for the transportation and electricity production in the neighborhood. It is assumed that all the hydrogen produced by the electrolysis system is stored in a reservoir connected to it. The amount of stored hydrogen, $x_{\mathrm{el}}(k)$, is a system state. The energy consumption of a typical electrolysis system, $u_{\mathrm{el}}(k)$, is a linear function of the produced hydrogen [23]. As a result, the stored hydrogen will increase due to hydrogen production of the electrolysis system with the amount of $\alpha_{\mathrm{el}} u_{\mathrm{el}}(k) T_{\mathrm{s}}$, where T_{s} is the sampling time interval and α_{el} is a constant related to the specifications of the system. Based on the CaPP microgrid scenario, all the fuel cell cars receive their fuel from the water electrolysis system, and hence, the PWA model of the system can be expressed as:

$$x_{\mathrm{el}}(k+1) = \begin{cases} x_{\mathrm{el}}(k) - \sum_{i=1}^{N_{\mathrm{veh}}} s_{\mathrm{r},i}(k) R_{\mathrm{f},i} & \text{if } s_{\mathrm{el}}(k) = 0 \\ x_{\mathrm{el}}(k) - \sum_{i=1}^{N_{\mathrm{veh}}} s_{\mathrm{r},i}(k) R_{\mathrm{f},i} + T_{\mathrm{s}} \alpha_{\mathrm{el}} u_{\mathrm{el}}(k) & \text{if } s_{\mathrm{el}}(k) = 1 \end{cases} , \quad (3)$$

where $s_{\mathrm{el}}(k)$ is the on/off switching signal of the electrolysis system. The operational constraints of the electrolysis system are presented in Appendix B.

3.3. Overall system model

The piecewise affine models of the cars and electrolysis system in (2) and (3) can be converted into mixed logical dynamical (MLD) models [24] by standard techniques [25]. An MLD model describes the behavior of a hybrid system including continuous and discrete variables. Based on Appendix C, this model is of the from:

$$\mathbf{x}(k+1) = \mathbf{x}(k) + B_1(k)\mathbf{u}(k) + B_3(k)\mathbf{z}(k) + B_4(k), \qquad (4)$$

where the system states and inputs are defined as:

$$\mathbf{x}(k) \triangleq \begin{bmatrix} \mathbf{x}_{\mathrm{f}}^T(k) & x_{\mathrm{el}}(k) \end{bmatrix}^T \qquad (5)$$

$$\mathbf{u}(k) \triangleq \begin{bmatrix} \mathbf{u}_{\mathrm{f}}^T(k) & \mathbf{s}_{\mathrm{r}}^T(k) & \mathbf{s}_{\mathrm{f}}^T(k) & u_{\mathrm{el}}(k) & s_{\mathrm{el}}(k) \end{bmatrix}^T. \qquad (6)$$

Here, a bold face variable indicates a vector containing the corresponding variables related to all cars. For example, $\mathbf{x}_{\mathrm{f}}(k) = \begin{bmatrix} x_{\mathrm{f},1}(k) & \dots & x_{\mathrm{f},N_{\mathrm{veh}}}(k) \end{bmatrix}^T$.

If we define $\omega(k)$ as the difference between the prediction of the residual electricity demand and its actual realization at time step k, matrices $G_1(k)$, $G_2(k)$, $G_3(k)$, and $G_4(k)$ can be determined in such a way that all the operational constraints given in Appendix A and B are included in the following inequality:

$$G_1(k)X(k) \le G_2(k) + G_3(k)\mathbf{x}(k) + G_4(k)\tilde{\omega}(k), \qquad (7)$$

where $X(k) = \begin{bmatrix} \tilde{\mathbf{u}}^T(k) & \tilde{\delta}_{\mathrm{exp}}^T(k) & \tilde{\mathbf{z}}^T(k) \end{bmatrix}^T$. Here, a variable with a tilde represents the stacked version of that variable in the prediction horizon. For example, $\tilde{\mathbf{u}}(k) = \begin{bmatrix} \mathbf{u}^T(k) & \dots & \mathbf{u}^T(k+N_{\mathrm{p}}-1) \end{bmatrix}^T$. Equation (4) with inequality (7) forms the MLD model of the overall system.

4. Control system operation

The proposed scenario assumes that, on the one hand, the wind turbine and PV systems are generating maximum power with respect to the weather situation, and on the other hand, the electricity load in the households is not controllable. The connection of the microgrid with the power grid allows the exchange of electricity, but it comes at a cost. An appropriate control system can help the microgrid to use the RES inside the neighborhood as much as possible and avoid unnecessary exchange of electricity. In addition, the physical limits in the transmission lines may cause a power unbalance inside the microgrid at some times. Fortunately, the presence of the fuel cell cars and the electrolysis system make it possible to still satisfy the power balance; this task is done via a central control system.

We assume that the central control system has access to weather forecast information, prediction of loads and renewable energy sources, predictions of the trip characteristics of the cars, and current values of the system states including the level of hydrogen stored in the electrolysis system and in each fuel cell car. The switching signals of fuel cell cars and electrolysis system, in addition to their power generation and consumption are determined by the control system in such a way that, firstly, the power balance is guaranteed in the system and, secondly, the operational costs of the system are minimized. To this end, a

model predictive control (MPC) algorithm is developed. In this algorithm, the operational costs of the system, subject to all constraints, are minimized by determining a sequence of control actions to be implemented in the future. The first control action is applied to the system and, at the next sample time, the whole procedure is repeated.

The following factors are considered to affect the operational costs:

- Switching the operation mode of the fuel cells and the electrolysis system, $J_{\mathrm{switch}}(k)$.

- Power generation of fuel cells and power consumption of the electrolyzer, $J_{\mathrm{power}}(k)$.

- The price of imported power, $J_{\mathrm{imp}}(k)$.

- The price of exported power, $J_{\mathrm{exp}}(k)$.

All the mentioned elements in the operational costs of the system create the cost function:

$$J(k) = J_{\mathrm{switch}}(k) + J_{\mathrm{power}}(k) + J_{\mathrm{imp}}(k) + J_{\mathrm{exp}}(k). \tag{8}$$

A more detailed description of the elements of the cost function is given in Appendix D.

By using the MLD model of the system derived in Section 3, the cost function can be written in the following form:

$$J(k) = W_{\mathrm{x}}(\tilde{\omega}(k))X(k) + W_{\mathrm{d}}(k)\tilde{\omega}(k) \tag{9}$$

The matrices $W_{\mathrm{x}}(\tilde{\omega}(k))$ and $W_{\mathrm{d}}(k)$ can be easily derived from the cost function by using the system model. Therefore, the optimization problem that the model predictive controller needs to solve at each time step is of the form:

$$\min_{X(k)} \max_{\tilde{\omega}(k)} \{J(k)\} \tag{10}$$

subject to (7).

The constraint of the optimization problem (10) should be satisfied for all possible realizations of $\tilde{\omega}(k)$, and hence, problem (10) is hard to solve in general. In order to simplify the problem, the uncertainty in the residual load of the neighborhood is assumed to be bounded.

Assumption 1: There exists a finite bound for the deviation of the predicted residual load from its actual value, $\omega(k)$, at each time step k. Therefore, it is possible to determine $\bar{\omega}$ and $\underline{\omega}$ such that for all k, $\underline{\omega} \leq \omega(k) \leq \bar{\omega}$.

With the assumption of bounded deviation of actual demand from the predicted values (Assumption 1) and using Lemma 1 to 3 in [26], the optimization problem can be formulated as an MILP problem as follows:

$$\min_{X(k)}\{\max\{W_{\mathrm{x}}(\tilde{\omega}_{\min}(k))X(k) + W_{\mathrm{d}}(k)\tilde{\omega}_{\min}(k), \ W_{\mathrm{x}}(\tilde{\omega}_{\max}(k))X(k) + W_{\mathrm{d}}(k)\tilde{\omega}_{\max}(k)\}\}$$

$$\tag{11}$$

subject to

$$G_1(k)X(k) \leq G_2(k) + G_3(k)\mathbf{x}(k) + G_4(k)\tilde{\omega}_{\min} \tag{12}$$

$$G_1(k)X(k) \leq G_2(k) + G_3(k)\mathbf{x}(k) + G_4(k)\tilde{\omega}_{\max}, \tag{13}$$

which can be solved by a variety of MILP solvers, such as GLPK [27], CPLEX [28], or Gurobi [29].

5. Simulation of a CaPP microgrid

In this section, the CaPP microgrid system described in Section 2 is simulated. A central controller is assumed to operate the system as described in Section 4. We consider 200 households inside the neighborhood. In order to simulate the electricity demand of the households, standard curves corresponding to 2014 are extracted from [30]. Using the standardized power fractions for each 15-min period of the year, we calculated the hourly demand by assuming a yearly consumption of 3,400 kWh/year [31]. Photovoltaic systems and wind turbines are the available RES in the system. It is assumed that the RES units generate the maximum electrical power that is possible given weather conditions. To simulate the power generation of the wind turbine, data from one of the measuring stations of the Dutch Institute of Meteorology is used [32]. Since the wind turbine is assumed to be in the community, a small turbine of 130kW is considered [33]. Given the turbine size, a measuring station in a coastal area is chosen to better capture the wind's energy [34]. Using the hourly wind speed data measured at Hoek van Holland in 2014, the hourly wind power is calculated for a 130kW turbine.

To simulate the power generation of solar photovoltaic systems, the PV Watts tool [35] is used. For the Netherlands, Amsterdam is the only location available in PV Watts. Hourly power generation of a 10 kWp PV system is calculated. The historical data show that the total RES capacity installed generate as much as 90% of the yearly electricity consumption in the neighborhood. However, considering the fact that the load of the microgrid is not controllable, only a part of the renewable energy is usable inside the microgrid.

As mentioned in Section 4, the residual load of the microgrid is assumed to be equal to the electricity load in the microgrid minus the power production of renewable energy sources. Figure 2 depicts the prediction of the residual load in the microgrid in a sample week. It is assumed that the prediction of the residual load contains uncertainty up to around 10 percent of its peak value. Here we assume that $\bar{\omega} = -\underline{\omega} = 10$ kW. The electrical connection between the microgrid and the power network are assumed to have a capacity of power exchange equal to 80 kW, i.e. $\bar{e}_{in} = -\underline{e}_{in} = 80$.
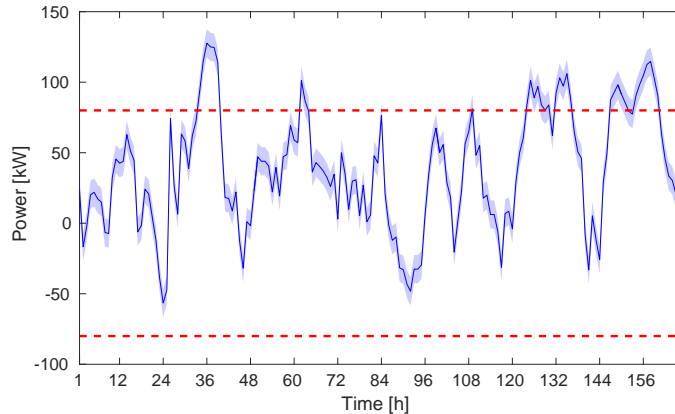

Figure 2: Residual load of the microgrid; shaded area indicates the uncertainty and the red lines are the limits on the power exchange between the microgrid and the power network.

The number of the fuel cell cars in the neighborhood is assumed to be 50. In order to derive the trip characteristics of the cars, the traveling behavior of the Dutch drivers for the year 2014 [36] is used. About 13,700 data points were used to derive the distribution of the departure and arrival times of the cars, and also the daily distance driven - for weekdays and weekends. The driving behaviors of the 50 cars are determined using these distributions. The resulting average daily distance traveled per car is 53 km. It is assumed that all the fuel cell cars consume 1 kg of hydrogen per 100 km driving distance. In addition, in the model of fuel cell stacks, the results of [21] are used to determine the required parameters. As a result, the parameters $\alpha_{f,i}$ and $\beta_{f,i}$ for all the cars are equal to 0.06 kg/kWh and 0.11 kg/h, respectively. The refilling speed of the cars, $R_{f,i}$, is assumed to be equal to 2 kg/h for all the cars. The maximum power generation of the fuel cells, $\bar{u}_{f,i}$, is set to 15 kW. Because the nominal power generation of a typical fuel cell car is around 100 kW, the fuel cell is operated at partial load. The coefficient of the power generation of fuel cell cars, W_{pf}, and power consumption of the electrolysis system, W_{pel}, in the cost function are assumed to be equal to 0.6 €/kW and 0.15 €/kW, respectively.

A water electrolysis system with a maximum power consumption of 100 kW and a hydrogen storage tank with the capacity of 500 kg are assumed to be available inside the neighborhood. The limits of the hydrogen level in the storage tank are $\underline{x}_{el} = 10$ kg and $\bar{x}_{el} = 500$ kg. For the water electrolysis system we assumed an efficiency of 70%. Considering that the high heating value of hydrogen is 39.4kWh/kg [23], α_{el} is equal to 0.02 kg/kWh.

The price of importing electricity is assumed to be equal to the price of the Amsterdam Power Exchange (APX) market in a day of April 2016 [37] and it is shown in Figure 3. In addition, we have considered a constant cost for the system, 0.2 €/kWh, to be paid to the grid operator in case of exporting electricity from the microgrid to the power network between 11 P.M. and 7 A.M. In this period of the time, the load of the power grid is low and exporting electricity from the microgrid to the power grid is discouraged.
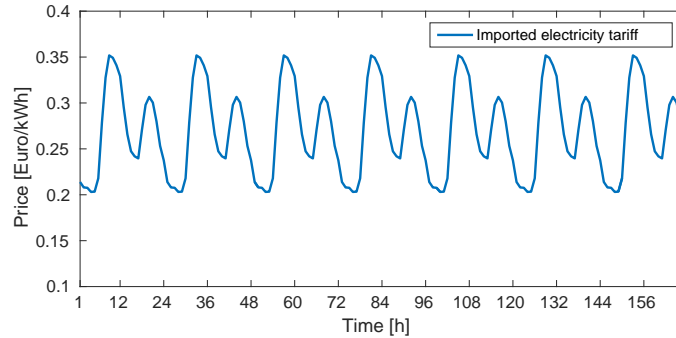

Figure 3: Price of importing electricity to the microgrid based on the APX market.

Based on the system model developed in Section 3 and the control algorithm of Section 4, the system is simulated for an entire year. Figure 4 illustrates the hydrogen level in the storage tank during a year. The use of hydrogen in the transportation and electricity generation by fuel cell cars causes the hydrogen level to fluctuate, but inside the predefined minimum and maximum of 10 and 500 kg, respectively.
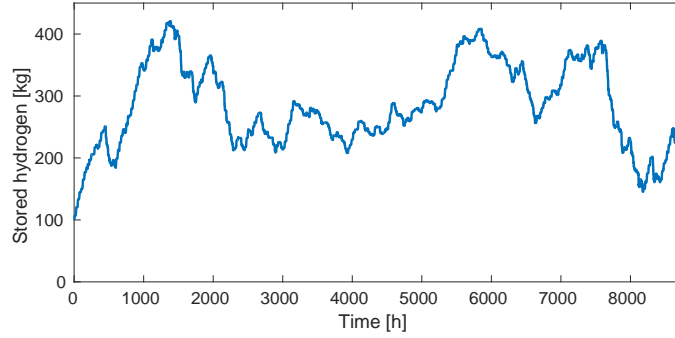
Figure 4: Level of hydrogen stored in the system.

If the renewable energy sources in the microgrid are operated with their maximum power generation capacity, the residual load of the microgrid would not be always in the range -80 to 80 kW, i.e. the range that exchange of power between the microgrid and the power network is possible. In addition, it is assumed that the power grid operator has set a price for exporting electricity from microgrid to the power network in order to discourage the microgrid from this action. The result of the simulation on the imported power to the microgrid in Figure 5(a) shows that the microgrid barely exports power to the power network. The residual load of the microgrid, depicted in Figure 2, indicates that in the absence of a water electrolysis system and in the case of avoiding the curtailment of the RES generation, the microgrid inevitably exports electricity to the power grid. However, Figure 5(a) shows that by using the fuel cell cars and the water electrolysis system, the imported power to the microgrid always remains inside the predefined bounds. Figure 5(b) represents the power consumption of the water electrolysis system in a sample week. The imported power to the microgrid is also influenced by the total power generation of fuel cell cars. Figure 5(c) shows the total power generation of the fuel cell cars inside the microgrid.

One may look at the microgrid as a medium of transferring electrical energy in which some sources supply energy to it and some others drain energy from it. Here, the electrical load of the households, the renewable energy sources, the fuel cell cars, and the water electrolysis system are the different sources connected to this medium for transferring electrical energy. In addition, we can assume that the power grid is another source of energy that can both inject energy to the microgrid or drain energy from it.

The simulation of the microgrid is now extended to an entire year and the resulting energy flows in the microgrid are listed in Table 1. It can be inferred from Table 1 that around 70% of the total consumed energy of the microgrid is delivered via the renewable energy sources, while the share of fuel cell cars in generation of the electrical energy of the microgrid is only 3%. Even though the fuel cell cars generate only a small portion of the total energy in the microgrid, they play an important role in decreasing the required capacity of the electrical connection between the power grid and the microgrid. The residual load of the microgrid has a peak power demand of around 170 kW and it repeatedly exceeds 150 kW. In the proposed control method it is guaranteed that even in the presence of uncertainty in the load and in the RES generation, the imported

11
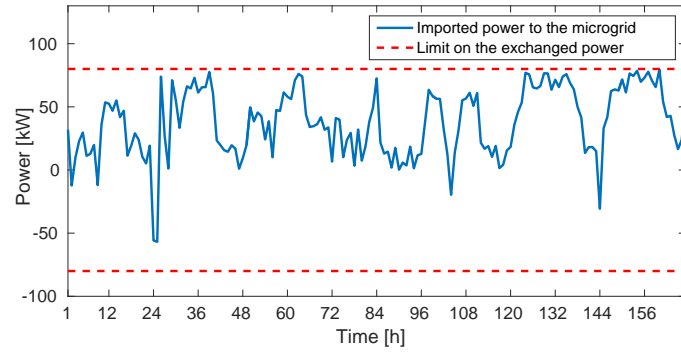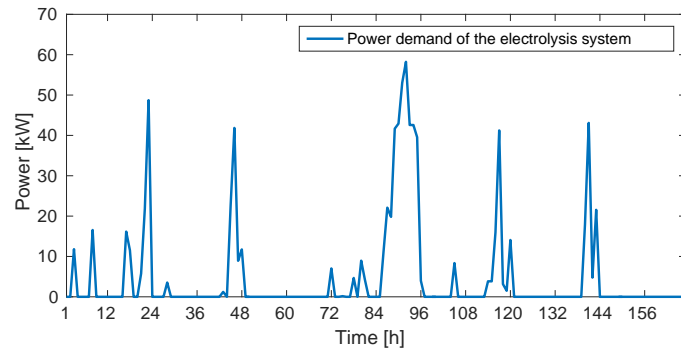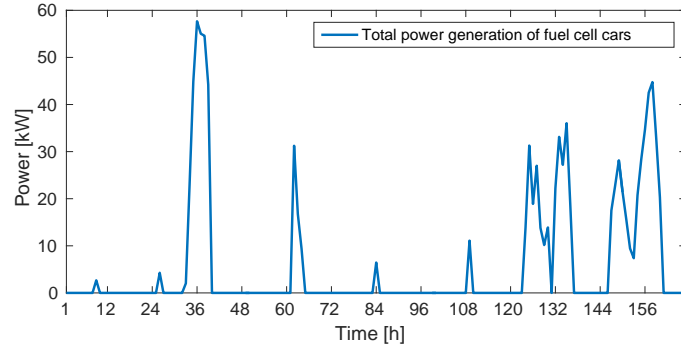
Figure 5: Operation of the control system during a week. (a) Imported power to the microgrid from the power grid. The red dashed lines indicate the limits on the exchanged power between the power grid and the microgrid. (b) Electrical power usage of the water electrolysis system. (c) Total power generation of fuel cell cars.

power to the microgrid does not exceed 80 kW. The reduction of the peak load in the microgrid is done using the fuel cell cars. Therefore, the presence of fuel cell cars plays an important role in reducing the peak of the imported power to the microgrid.

Table 1: Electrical energy generation and consumption in one year

Electrical energy load/source	Generation [MWh]	Consumption [MWh]
Power grid	227	74
Households	0	680
Renewable energy	607	0
Fuel cell cars	24	0
Water electrolysis system	0	103

6. Conclusions

The presence of the FCEVs and the water electrolysis system in a microgrid creates the flexibility for the microgrid to store energy in the form of hydrogen and to regenerate electricity from the stored hydrogen. In the scenario developed in this paper, hydrogen is the storage form of energy and it is used both for the transportation of the cars and for the generation of electricity. Our assumption is that RES can generate electricity with their maximum capacity and the fast variation in the power generation of RES is compensated inside the microgrid. As a result, the problem of congestion in the power network and fast variation in the power generation profile of the conventional power plants can be solved without curtailment in the RES generation. The tariff on power exchange between the microgrid and the power network influence the decision of the microgrid controller to export or import power from the power network. The influence of the power exchange tariff on the performance of the microgrid is a topic for future research. The simulation of the CaPP microgrid system illustrates the effectiveness of the developed control system.

In the system presented in this paper, surplus renewable generation in the microgrid is stored in the form of hydrogen. Therefore, in the formulated scenario of a congested network the microgrid does not cause additional problems to the larger grid. By making this hydrogen available for transportation purposes and for re-electrification, the use of FCEVs can reduce the well-to-wheel emissions in the transport system as well as the carbon emissions related to power generation within the neighborhood. Further possibilities for synergies between hydrogen and electricity networks can be explored in other scenarios, such as one in which such a microgrid becomes a net producer of electricity in relation to the main grid.

Appendix A: Full description of the fuel cell cars model

Here we explain the structure and terms of (2) and its five modes. The first mode indicates the refilling process. The system enters this mode when the car is available for power generation and the value of $s_{r,i}(k)$ is set to 1 by the controller. During this mode, the fuel level of the car increases with a constant rate $R_{f,i}$. The second and the third modes belong to the situation when the car is inside the neighborhood and it is not refilled. In the second mode the fuel cell stack is turned off, and hence, the amount of fuel in the car does not change in time. The third mode represents the system dynamics when the fuel cell stack is turned on and the net power production is equal to $u_{f,i}(k)$. The last two modes in (2) belong to the situation where the car has left the neighborhood. A fuel cell car is not allowed to be refilled or to generate electricity when it is not inside the neighborhood and as a result, the fuel level $x_{f,i}(k)$ does not influence the system dynamics in this case. We can assume that the fuel level remains constant during the absence of the car and that one sample time before arrival of the car in the neighborhood, all the fuel used in the transportation is subtracted from the initial value.

It is assumed that the refilling process and the generation of electricity by a car can be done only when the car is inside the neighborhood. In other words,

$$\text{if} \quad \lambda_{f,i}(k) = 0 \quad \text{then} \quad s_{r,i}(k) = 0. \tag{14}$$

$$\text{if} \quad \lambda_{f,i}(k) = 0 \quad \text{then} \quad s_{f,i}(k) = 0. \tag{15}$$

In addition, we assume that during the refilling process, the fuel cell stack should be turned off. Therefore, another constraint in the system is given by:

$$\text{if} \quad s_{r,i}(k) = 1 \quad \text{then} \quad s_{f,i}(k) = 0. \tag{16}$$

Based on the physical limits, an upper bound exists for the generation of electricity in each fuel cell stack. In addition, the rate of power generation is limited to an upper and lower bound as follows:

$$0 \leq u_{f,i}(k) \leq \bar{u}_{f,i} \tag{17}$$

$$\Delta \underline{u}_{f,i} \leq \Delta u_{f,i} \leq \Delta \bar{u}_{f,i}. \tag{18}$$

The fuel cell stack cannot generate electricity when it is turned off, i.e.,

$$\text{if} \quad s_{f,i}(k) = 0 \quad \text{then} \quad u_{f,i}(k) \leq 0. \tag{19}$$

The inequality (19) combined with (17) implies that whenever a fuel cell is turned off, the power generation of that fuel cell has to be equal to zero.

The maximum level of fuel in each car is indicated by $\bar{x}_{f,i}$ and the minimum level of fuel that is necessary for the next travel of car is indicated by $\underline{x}_{f,i}(k)$. If the amount of fuel in a car is equal to or lower than this minimum level necessary for the travel purpose, the car is not used in the task of power generation. Therefore:

$$\text{if} \quad x_{f,i}(k) \leq \underline{x}_{f,i}(k) \quad \text{then} \quad s_{f,i}(k) = 0. \tag{20}$$

As a result, the constraints on $x_{f,i}(k)$ can be written as:

$$\underline{x}_{f,i}(k)s_{f,i}(k) \leq x_{f,i}(k) \leq \bar{x}_{f,i}. \tag{21}$$

Appendix B: Constraints on the operation of the electrolysis system

The physical limitations of the system dictate a bound on the stored hydrogen, consumed electricity and its rate of change as follows:

$$\underline{u}_{\text{el}} \leq u_{\text{el}}(k) \leq 0 \tag{22}$$

$$\Delta\underline{u}_{\text{el}} \leq \Delta u_{\text{el}}(k) \leq \Delta\bar{u}_{\text{el}} \tag{23}$$

$$\underline{x}_{\text{el}} \leq x_{\text{el}}(k) \leq \bar{x}_{\text{el}} \tag{24}$$

The electrolysis system consumes electricity only when it is turned on. Therefore,

$$\text{if} \quad s_{\text{el}}(k) = 0 \quad \text{then} \quad u_{\text{el}}(k) \geq 0. \tag{25}$$

The inequality (25) combined with (22) implies that whenever $s_{\text{el}}(k) = 0$, then $u_{\text{el}}(k) = 0$.

Appendix C: Intermediate steps in deriving the MLD model

To derive the MLD model, we define a binary auxiliary variable $\delta_{\text{exp}}(k)$ that indicates whether electricity is imported or exported from the microgrid to the power network at time step k. If we define $e_{\text{in}}(k)$ as the imported power to the system, the value of $\delta_{\text{exp}}(k)$ is determined as follows:

$$e_{\text{in}}(k) \leq 0 \Leftrightarrow \delta_{\text{exp}}(k) = 1. \tag{26}$$

We define a lower, $\underline{e}_{\text{in}}$, and an upper bound, $\bar{e}_{\text{in}}$, for the imported power to the microgrid, $e_{\text{in}}(k)$. Based on the physical properties of the electrical networks, the amount of imported power to the microgrid is given by:

$$e_{\text{in}}(k) = P_{\text{d}}(k) + \omega(k) - u_{\text{el}}(k) - \sum_{i=1}^{N_{\text{veh}}} u_{\text{f},i}(k). \tag{27}$$

Therefore, the following constraint exists in the system:

$$\underline{e}_{\text{in}} \leq P_{\text{d}}(k) + \omega(k) - u_{\text{el}}(k) - \sum_{i=1}^{N_{\text{veh}}} u_{\text{f},i}(k) \leq \bar{e}_{\text{in}}, \tag{28}$$

where $P_{\text{d}}(k)$ is the prediction of residual electrical load in the microgrid, which is equal to the total power production of the renewable energy sources subtracted from the load demand in the microgrid. The difference between the prediction of residual electricity demand and its actual realization at time step k is an uncertain value that is denoted by $\omega(k)$.

Using the models (2) and (3), the overall system model can be written as (4), where $\mathbf{z}(k)$ contains the continuous auxiliary variables that are used in the MLD models [24]. The matrices $B_1(k)$, $B_3(k)$, and $B_4(k)$ are time-varying, but because we can predict the trip characteristics of the cars, they can be determined over the whole prediction horizon.

All the mentioned constraints in the model of the fuel cell cars, the electrolysis system and the definition of auxiliary variables are affine with respect to

the variables $\mathbf{x}(k)$, $\mathbf{u}(k)$, $\delta_{\exp}(k)$, $\mathbf{z}(k)$, and $\omega(k)$. Therefore, for each sample time we can express the inequalities as:

$$E_1\mathbf{u}(k) + E_4\mathbf{x}(k) + E_{51}(k) + E_{52}\omega(k) \geq E_2\delta_{\exp}(k) + E_3\mathbf{z}(k). \qquad (29)$$

Using (4) and defining $G_1(k)$, $G_2(k)$, $G_3(k)$, and $G_4(k)$ in an appropriate way, the whole set of constraints for all the prediction horizon can be written in the form (7).

Appendix D: Description of the cost function

The different parts of the cost function are:

$$J_{\text{switch}}(k) = \sum_{j=0}^{N_{\text{p}}-1} \left(\sum_{i=1}^{N_{\text{veh}}} W_{\text{sf}}|\Delta s_{\text{f},i}(k+j)| + W_{\text{sel}}|\Delta s_{\text{el}}(k+j)| \right) \qquad (30)$$

$$J_{\text{power}}(k) = \sum_{j=0}^{N_{\text{p}}-1} \left(\sum_{i=1}^{N_{\text{veh}}} W_{\text{pf}}u_{\text{f},i}(k+j) + W_{\text{pel}}u_{\text{el}}(k+j) \right) \qquad (31)$$

$$J_{\text{imp}}(k) = \sum_{j=0}^{N_{\text{p}}-1} C_{\text{e,imp}}(k+j)e_{\text{in}}(k+j)(1 - \delta_{\exp}(k+j)) \qquad (32)$$

$$J_{\exp}(k) = \sum_{j=0}^{N_{\text{p}}-1} C_{\text{e,exp}}(k+j)(-e_{\text{in}}(k+j))\delta_{\exp}(k+j), \qquad (33)$$

and they can be interpreted as follows:

- $J_{\text{switch}}(k)$: This part of the cost function is used to include the strong effect of switching the operation mode of fuel cells and electrolysis systems on their life time. A term $W_{\text{sf}}|\Delta s_{\text{f},i}(k)|$ is considered for each fuel cell car i as the cost of switching at time step k, where W_{sf} is a weight factor to determine the importance of the degradation in the whole operational cost. A similar term, $W_{\text{sel}}|\Delta s_{\text{el}}(k)|$, is considered for the electrolysis system.

- $J_{\text{power}}(k)$: This term reflects the operational costs, related to the power generation of fuel cells or power consumption of water electrolysis system. The price of hydrogen per kilogram, which is used by the fuel cells or is produced by the electrolysis system, are influencing the constant coefficients W_{pf} and W_{pel}.

- $J_{\text{imp}}(k)$: It is assumed that the price of imported electricity should be paid to the power grid operator. As a result, the imported power affects the operational costs of the microgrid. If $C_{\text{e,imp}}(k+j)$ represents the price of electricity at time step $k+j$, the term $\sum_{j=0}^{N_{\text{p}}-1} C_{\text{e,imp}}(k+j)e_{\text{in}}(k+j)(1 - \delta_{\exp}(k+j))$ indicates the price of imported power, where $(1 - \delta_{\exp}(k+j))$ determines whether the electricity is imported or not.

- $J_{\exp}(k)$: In order to control the total power generation in the power grid, the amount of injected power to the grid should be controlled. When extra power can be used in the power grid, for example the peak demand hours, the grid operator pays the microgrid to inject electricity to the network.

However, the scenario assumes that the neighborhood can be seen as a load, and not a generation unit, from the power network's point of view. Therefore, the injection of power to the power grid is penalized by an amount $C_{\mathrm{e,exp}}(k)$ at time step k.

References

[1] H. Holttinen, A. Tuohy, M. Milligan, E. Lannoye, V. Silva, S. Müller, L. Söder, The flexibility workout: Managing variable resources and assessing the need for power system modification, IEEE Power and Energy Magazine 11 (6) (2013) 53–62.

[2] M. Wolsink, The research agenda on social acceptance of distributed generation in smart grids: Renewable as common pool resources, Renewable and Sustainable Energy Reviews 16 (1) (2012) 822–835.

[3] R. A. Verzijlbergh, Z. Lukszo, M. D. Ilic, Comparing different EV charging strategies in liberalized power systems, in: Proceedings of the International Conference on the European Energy Market, 2012, pp. 1–8.

[4] W. Kempton, J. Tomić, Vehicle-to-grid power implementation: From stabilizing the grid to supporting large-scale renewable energy, Journal of Power Sources 144 (1) (2005) 280–294.

[5] T. E. Lipman, J. L. Edwards, D. M. Kammen, Fuel cell system economics: comparing the costs of generating power with stationary and motor vehicle PEM fuel cell systems, Energy Policy 32 (1) (2004) 101–125.

[6] J. Kissock, Combined heat and power for buildings using fuel-cell cars, in: Proceedings of the ASME International Solar Energy Conference, 1998, pp. 121–132.

[7] A. J. M. van Wijk, L. Verhoef, Our Car as Power Plant, Delft University Press, 2014.

[8] A. Fernandes, T. Woudstra, A. van Wijk, L. Verhoef, P. V. Aravind, Fuel cell electric vehicle as a power plant and SOFC as a natural gas reformer: An exergy analysis of different system designs, Applied Energy 173 (2016) 13–28.

[9] Z. Lukszo, E. H. Park Lee, Demand Side and Dispatchable Power Plants with Electric Mobility, in: A. Beaulieu, J. de Wilde, M. A. J. Scherpen (Eds.), Smart Grids from a Global Perspective: Bridging Old and New Energy Systems, Springer International Publishing, 2016, pp. 163–177.

[10] S. Parhizi, H. Lotfi, A. Khodaei, S. Bahramirad, State of the art in research on microgrids: A review, IEEE Access 3 (2015) 890–925.

[11] H. Khodr, N. El Halabi, M. García-Gracia, Intelligent renewable microgrid scheduling controlled by a virtual power producer: A laboratory experience, Renewable Energy 48 (2012) 269–275.

[12] C. Battistelli, Generalized microgrid-to-smart grid interface models for vehicle-to-grid, in: 2013 IEEE PES Innovative Smart Grid Technologies Conference, 2013, pp. 1–6.

[13] K. Shinoda, E. Park Lee, M. Nakano, Z. Lukszo, Optimization model for a microgrid with fuel cell vehicles, in: 13th IEEE International Conference on Networking, Sensing and Control (ICNSC), 2016.

[14] M. Korpås, A. T. Holen, Operation planning of hydrogen storage connected to wind power operating in a power market, IEEE Transactions on Energy Conversion 21 (3) (2006) 742–749.

[15] L. Bolívar Jaramillo, A. Weidlich, Optimal microgrid scheduling with peak load reduction involving an electrolyzer and flexible loads, Applied Energy 169 (2016) 857–865.

[16] M. Petrollese, L. Valverde, D. Cocco, G. Cau, J. Guerra, Real-time integration of optimal generation scheduling with MPC for the energy management of a renewable hydrogen-based microgrid, Applied Energy 166 (2016) 96–106.

[17] J. M. Vidueira, A. Contreras, T. N. Veziroglu, PV autonomous installation to produce hydrogen via electrolysis, and its use in FC buses, International Journal of Hydrogen Energy 28 (9) (2003) 927–937.

[18] A. Parisio, E. Rikos, L. Glielmo, A model predictive control approach to microgrid operation optimization, IEEE Transactions on Control Systems Technology 22 (5) (2014) 1813–1827.

[19] A. Parisio, L. Glielmo, Stochastic model predictive control for economic/environmental operation management of microgrids, in: European Control Conference (ECC), Zürich, Switzerland, 2013, pp. 2014–2019.

[20] C. A. Hans, V. Nenchev, J. Raisch, C. Reincke-Collon, Minimax model predictive operation control of microgrids, in: 19th World Congress of the International Federation of Automatic Control, Cape Town, South Africa, 2014, pp. 10287–10292.

[21] P. Rodatz, G. Paganelli, A. Sciarretta, L. Guzzella, Optimal power management of an experimental fuel cell/supercapacitor-powered hybrid vehicle, Control Engineering Practice 13 (2005) 41–53.

[22] F. Alavi, N. van de Wouw, B. De Schutter, Min-max control of fuel-cell-car-based smart energy systems, in: European Control Conference, Aalborg, DK, 2016.

[23] J. Ivy, National Renewable Energy Laboratory, Summary of electrolytic hydrogen production: Milestone completion report, National Renewable Energy Laboratory, 2004.

[24] A. Bemporad, M. Morari, Control of systems integrating logic, dynamics, and constraints, Automatica 35 (3) (1999) 407–427.

[25] W. P. M. H. Heemels, B. De Schutter, A. Bemporad, Equivalence of hybrid dynamical models, Automatica 37 (7) (2001) 1085–1091.

[26] F. Alavi, E. Park Lee, N. van de Wouw, B. De Schutter, Z. Lukszo, Fuel cell cars in a microgrid for synergies between hydrogen and electricity networks – addendum, Tech. Rep. 16-008a, Delft Center for Systems and Control, Delft University of Technology, Delft, The Netherlands (Apr. 2016).

[27] GLPK (GNU Linear Programming Kit).
URL https://www.gnu.org/software/glpk/

[28] CPLEX optimizer.
URL http://www-01.ibm.com/software/commerce/optimization/cplex-optimizer/

[29] Gurobi optimization.
URL http://www.gurobi.com/

[30] Energie Data Services Nederland (EDSN), Verbruiksprofielen - profielen elektriciteit 2014 (Load profiles - electricity profiles 2014) (in Dutch) (2015).
URL http://nedu.nl/portfolio/verbruiksprofielen/

[31] E. Veldman, M. Gaillard, M. Gibescu, J. Slootweg, W. Kling, Modelling future residential load profiles, in: Innovation for Sustainable Production, 2010, pp. 64–68.

[32] Royal Netherlands Meteorological Institute (KNMI), Uurgegevens van het weer in Nederland (Hourly weather data in the Netherlands) (in Dutch) (2015).
URL http://knmi.nl/nederland-nu/klimatologie/uurgegevens

[33] U.S. Department of Energy, Wind and water program: Community wind benefits (November 2012).
URL http://www.nrel.gov/docs/fy13osti/56386.pdf

[34] Milieu Centraal, Kleine windmolens ("Small wind turbines") (in Dutch) (2016).
URL https://www.milieucentraal.nl/klimaat-en-aarde/energiebronnen/windenergie/kleine-windmolens/

[35] National Renewable Energy Laboratory, PVWatts Calculator (2015).
URL http://pvwatts.nrel.gov/pvwatts.php

[36] Centraal Bureau voor de Statistiek (CBS), Rijkswaterstaat (RWS), Onderzoek Verplaatsingen in Nederland 2014 (Research on Movements in the Netherlands 2014) - Data Archiving and Networked Services (in Dutch) (2015).
URL https://easy.dans.knaw.nl/

[37] Amsterdam Power Exchange, APX Market Results - APX Power NL Day Ahead (April 2016).
URL http://apxgroup.com/market-results/apx-power-nl